Chapter 6

Technological Aspects of Production and Processing of Functional Materials Based on Intermetallic Fe-Al

Magdalena Jabłońska, Iwona Bednarczyk,
Anna Śmiglewicz and Tomasz Mikuszewski

Additional information is available at the end of the chapter

http://dx.doi.org/10.5772/intechopen.76701

Abstract

The problems of this paper relate to a possibility to affect the structure and properties of new alloys with an intermetallic phase matrix of the Fe-Al system by improvements in casting and hot plastic working processes. The studies were focused on selection of an optimum chemical composition and parameters of the casting and heat treatment processes for further hot plastic working process. The primary goal was to obtain semi-finished products in the forms of sheets and bars with specified set of mechanical and physical properties. The works included several selected alloys with various Al content and variable contents of alloying elements influencing the formation of intermetallic phases. A series of characteristics of mechanical, physical, and chemical properties of alloys containing 28 and 38% of Al were developed. The result of the work consists in the development of a technology for hot forming of flat and round products.

Keywords: Fe-Al intermetallics, structure ordering, vacancy hardening, plastic working, microstructure

1. Introduction

Fe-Al alloys with an ordered solid solution structure belong to the group of modern heat-resistant engineering materials with favorable physicochemical and mechanical properties at elevated and high temperature [1, 2]. The properties of Fe-Al alloys, such as low density, high melting point, high strength, and good oxidation resistance, combined with fracture toughness, create broad perspectives for industrial applications [3, 4]. These properties are the result of the existing ordering of the crystal structure, which reduces the free energy of the ordered alloys

and thus their greater durability. In addition, alloys from the Fe-Al system are characterized by high fatigue strength [5]. Particular properties of alloys from the Fe-Al system make them a favorable material used for construction, as an alternative for stainless steels containing expensive alloying elements and for superalloys, as a coating material, as a material for elements operating under high-temperature corrosion, and as a starting material for complex alloys and composites [1–7]. Their application options are oriented toward filling the gap between the currently used conventional steels having particular properties and nickel superalloys in manufacturing of products for aircraft, automotive, and power industries. Despite many advantages of the Fe-Al alloys, their practical use is limited by their low creep strength at high-temperature, insufficient plasticity at moderate and low temperatures, as well as susceptibility to brittle cracking at room temperature [2–6, 8–15]. In some cases long-range ordering occurring in these alloys, on the one hand, limits the use of typical processing technologies such as cold plastic working and, on the other hand, provides a set of unique mechanical, physical, and chemical properties. According to the Fe-Al phase equilibrium system (**Figure 1**) [14], aluminum dissolves with iron α up to 54 at.% at 1102°C and 48 at.% at a temperature of about 200°C. During cooling, the constant limit solution Al in Fe is changed to the order Fe-Al. Further cooling affects to replace superstructure Fe-Al into the superstructure of Fe_3Al.

For alloys from the Fe-Al system, the most important factors affecting their properties are aluminum content and the content of alloy microadditions. Fe-Al alloys show an increase in the yield stress with an increase of Al content. Two groups of alloying additives can be distinguished in Fe-Al alloys due to their effect:

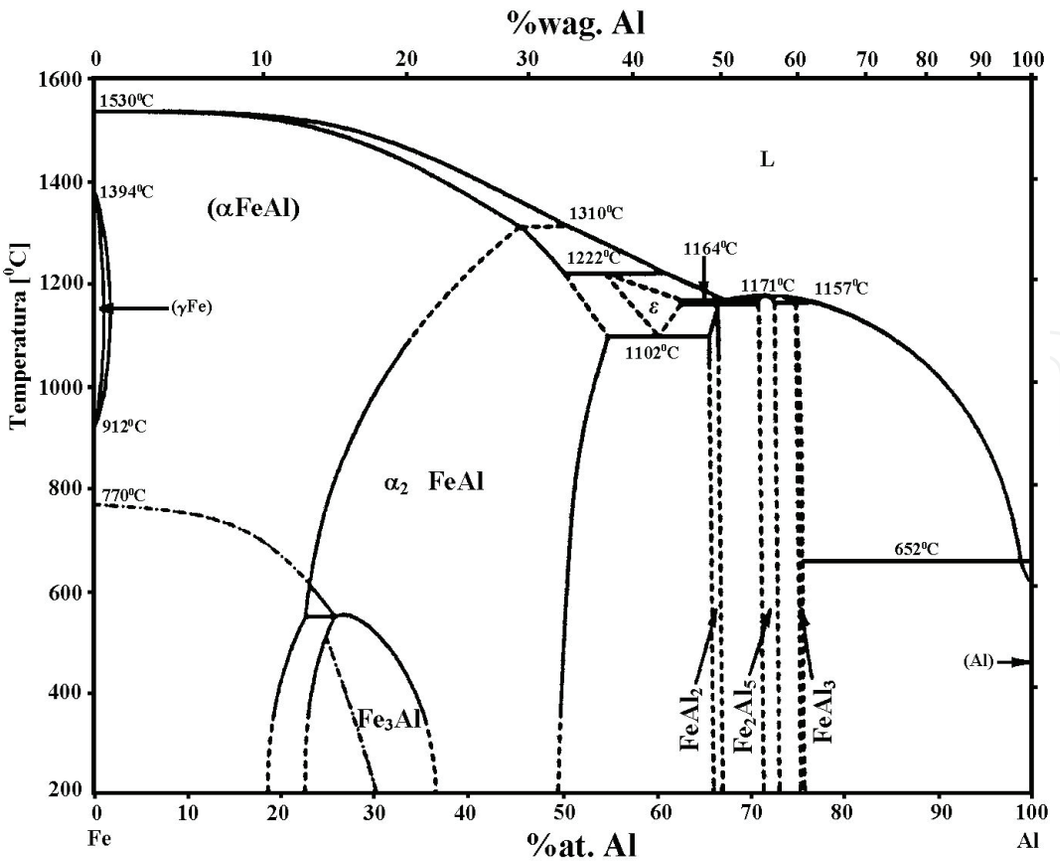

Figure 1. Fe-Al system.

http://dx.doi.org/10.5772/intechopen.76701

1. Additives forming separations that affect the increase of strength. These include Nb, Zr, B, C, Cu and Ta.
2. Alloy additions affecting the strengthening of the solid solution, which may include Cr, Ti, Mn, Si, Mo, V, and Ni.

Fe-Al-based alloys have the highest concentration of thermal vacancies as the only of the long-range intermetallic alloy group. Their presence exerts influence on mechanical properties and, as a result, on the possibilities of industrial-scale application. The concentration of vacancies in Fe-Al alloys increases with the increase of Al content. Alloy additions, such as Cu, Ni, Mn, Cr, V, and Ti, which increase the hardness, affect the slight increase in the concentration of thermal vacancies; however, the addition of B is significant here because it affects the acceleration of the elimination of vacancies. At low temperatures, triple defects and their diffusion dominate by jumping the Fe atoms to the Al subnet. Then, the process of pushing back the anti-position Fe atoms from the Al subnet to the Fe network takes place. At a higher temperature, double vacancies are formed, and their movement is made by double jumps. The increase in the concentration of vacancies causes the increase of the yield stress [16–18].

Time perspective of application of this group of materials depends particularly on thorough understanding of the dependence between, on the one hand, the production processes and the microstructure, and on the other hand, physical properties, such as thermal conductivity and thermal expansion, phase transition temperatures, and defecting and structural ordering of these compounds [18–28]. Such an approach will provide a range of information which allows for anticipating ways of influencing the process plasticity of these alloys.

2. Characteristics of the material for studies

Binary and complex alloys from the Fe-Al system (**Table 1**) were the materials for studies. An analysis of available Fe-Al and Fe-Al-Me equilibrium systems and literature research indicate that the chemical composition of alloys for plastic working should be in the range of 25% at. Al to 60% at. Al, and it may contain additives such as molybdenum, zirconium, carbon, and boron, with contents in the following ranges (at.%): Mo (0.2 ± 0.1), Zr (0.1 ± 0.05), C (0.1 ± 0.1),

Alloy	Al	Mo	Zr	C	B	Cr	Fe	HV2
Fe-28Al	28.0	–	–	–	–	–	72.0	299
Fe-28Al-5Cr	28.0	–	–	–	–	5.0	67.0	240
Fe-38Al	38.0	–	–	–	–	–	62.0	287
Fe-38Al-5Cr	38.0	–	–	–	–	5.0	57.0	213
Fe-28Al+microadd.	28.0	0.2	0.05	0.10	0.01	–	71.64	303
Fe-28Al-5Cr+microadd.	28.0	0.2	0.05	0.10	0.01	5.0	66.64	266
Fe-38Al+microadd.	38.0	0.2	0.05	0.10	0.01	–	61.64	281

Table 1. Chemical composition of the obtained alloys (at.%) and their hardness after heat treatment at 1000°C/24 h and furnace-cooling.

and B (0.02 ± 0.01). Most of all, the indicated microadditions serve the purpose of strengthening of grain boundaries, as well as grain refining.

An analysis of chemical composition carried out by optical emission spectrometry (OES) confirmed obtaining chemical compositions assumed for melting.

3. Results of experiments

3.1. Preparation of alloys with varied contents of Al, Fe, alloying elements, and microadditions

Currently, the alloys from the Fe-Al system used as casting materials do not pose major technological problems during melting and casting. However, the requirements set for these alloys increase if semifinished products intended for a further processing are manufactured from them. Such alloys must exhibit a set of features ensuring their technological plasticity, including high-purity, uniform, and fine-grained structure with a minimal level of casting defects such as shrinkage porosities, cracks, and microporosity. Melting was carried out using a conventional melting technique in an IS5/III induction vacuum furnace from Leybold-Heraeus, using a compacted magnesia crucible (from $MgO{\cdot}Al_2O_3$ spinel) with a granulation of 0.05–2 mm, under a vacuum of 13.5 Pa. Melting of alloys under vacuum allows for avoiding the use of protective covers and refiners and enables to use pure metals instead of master alloys as charges. It also promotes alloy degassing and protects from oxidation, but it requires taking into account the melting loss of the components in the result of their evaporation. The following constituents were used during the melting process: as charge components (ARMCO iron, aluminum of 99.98 wt.% purity, electrolytic chromium) and as microadditions (technically pure molybdenum in the form of a compressed powder, technically pure iodine zirconium, crystalline boron, carbon in the form of anthracite). Due to the form of the charge materials, the melting loss was assumed for molybdenum, zirconium, carbon, and boron. Mechanically, purified and dried pieces of the main alloy components, i.e., iron and aluminum, were placed together in the crucible. After melting and homogenization, the charge was overheated to a temperature of approx. 1600°C, and the following microadditions were added to the melt: zirconium, molybdenum, carbon, and boron. After reducing the temperature to approx. 1530÷1550°C and maintaining it for homogenization and degassing, the alloy was cast. After melting, the alloys were remelted once. Preparation of casts both having circular (the so-called bars) and rectangular (the so-called flats) cross sections was planned. The alloys were cast under the same conditions into cold graphite molds (**Figure 2**). In the upper sections of the mold, double insulating felt with a thickness of 3÷4 cm was used, serving the purpose of protection from rapid solidification of the liquid metal. **Figures 1–4** show the applied graphite molds and dimensions of the obtained ingots.

The alloys after casting were characterized by a coarse-grained structure. In the case of the alloys without microadditions, occurrence of grains with diversified dimensions was observed, while in the alloys containing microadditions, the shape of the grains is typical for a primary dendritic structure. In **Figure 3**, selected microstructures of the studied alloys after homogenizing at 1000°C for 24 h and furnace-cooling are shown. In the alloys not containing

http://dx.doi.org/10.5772/intechopen.76701

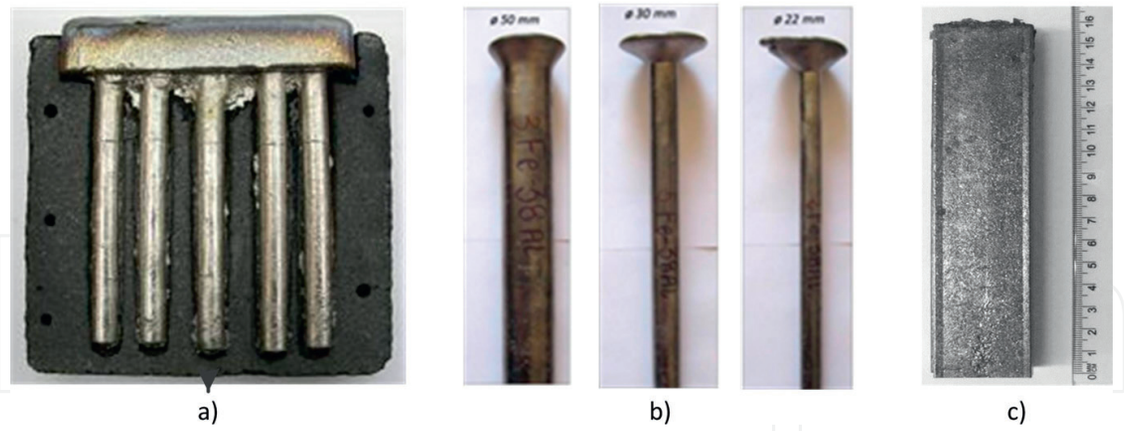

Figure 2. Graphite mold for ingots having dimensions (a) Ø12 mm, l = 120 mm, (b) l = 45 mm and diameters (a) Ø50 mm, (b) Ø30 mm, and (c) Ø22 mm, (c) of approx. 160 mm × 30 mm × 20 mm.

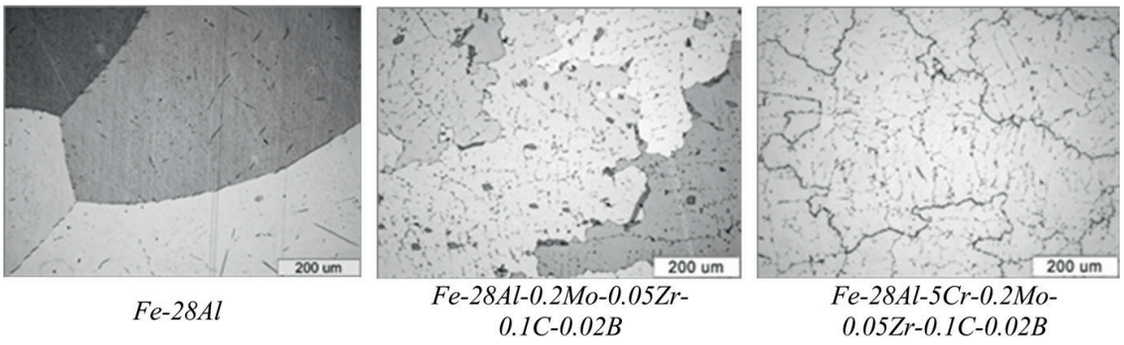

Figure 3. Microstructures of the alloys after annealing 1000°C/24 h/furnace.

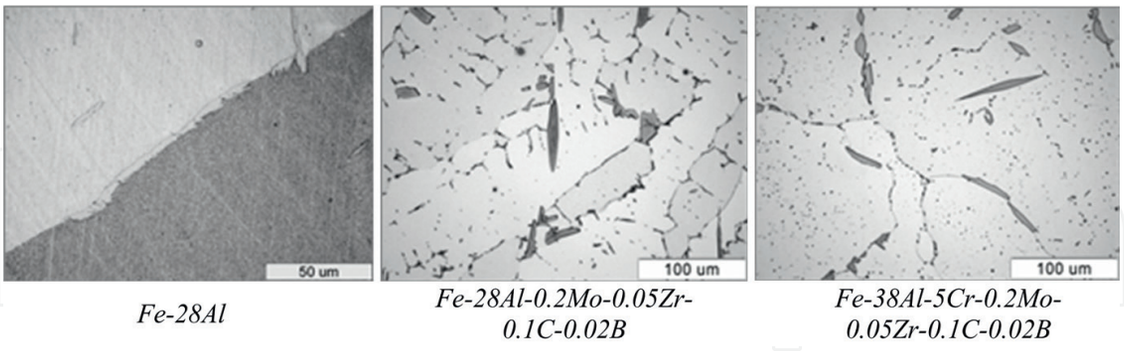

Figure 4. Microstructures of the alloys after annealing 1000°C/24 h/furnace. The presence of phases inside the grains and at their boundaries.

the Cr alloying element, both binary (Fe-28Al, Fe-38Al) and complex (Fe-28Al-0.2Mo-0.05Zr-0.1C-0.02B, Fe-38Al-0.2Mo-0.05Zr-0.1C-0.02B) occurrence of precipitations both at the grain boundaries and inside the grains was found (**Figure 3**).

To identify the precipitations found in the studied alloys, investigations using scanning electron microscopy (SEM), scanning transmission electron microscopy (STEM), and transmission electron microscopy (TEM) were carried out. Non-etched and etched samples were

examined. Due to the fact that phases of the same type were found in the Fe-28Al, Fe-28Al-0.2Mo-0.05Zr-0.1C-0.02B, Fe-38Al, and Fe-38Al-5Cr-0.2Mo-0.05Zr-0.1C alloys, the phase identification results are presented for the Fe-28Al alloy only. The results of qualitative and quantitative analyses of chemical composition for the Fe-28Al alloy are presented in **Figure 5**.

The results of studies of chemical composition microanalysis obtained by scanning electron microscopy (analysis in microzones and surface distribution of the elements) indicate

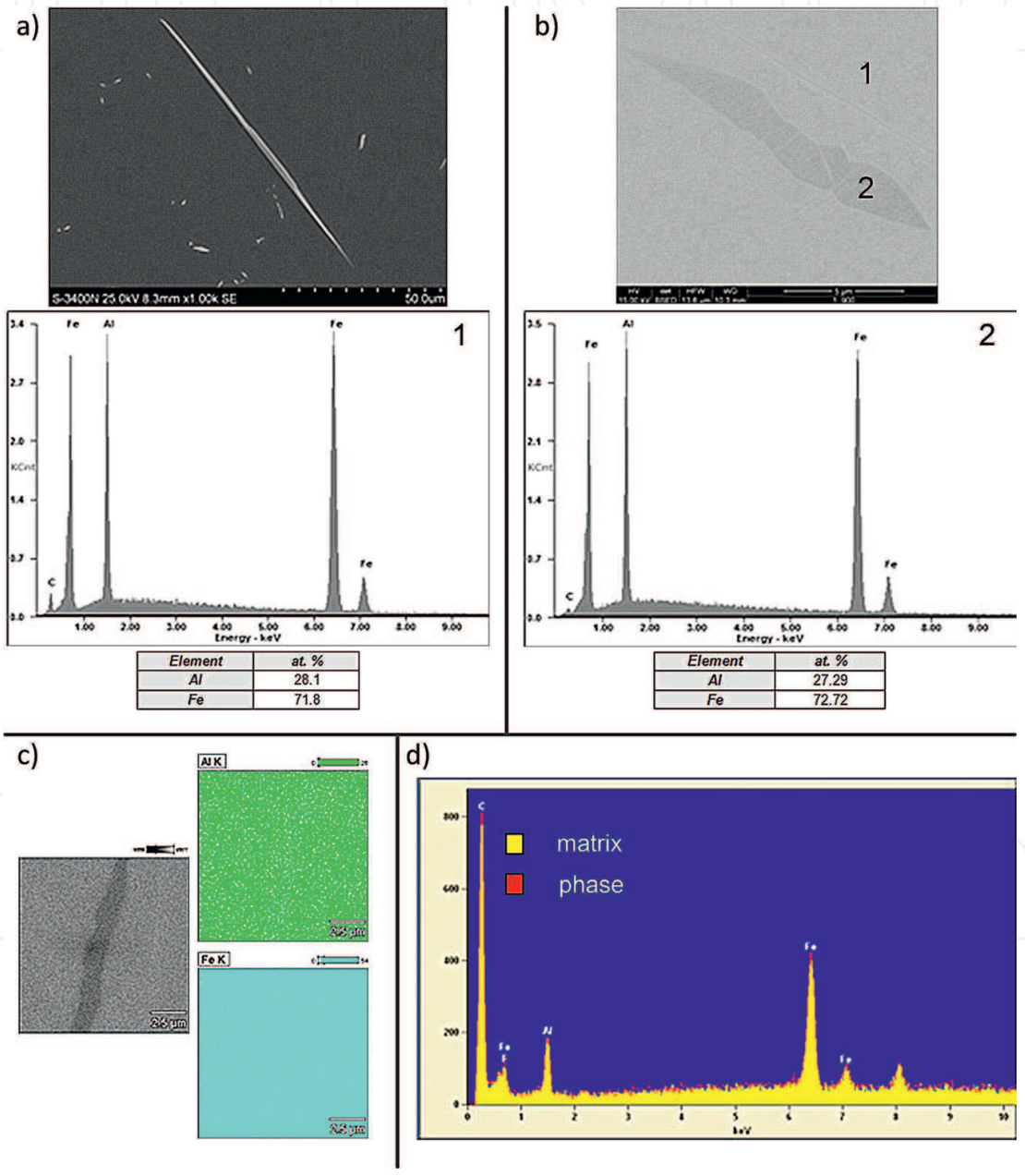

Figure 5. Results of microstructure studies (SEM, STEM) and analysis of chemical composition together with the X-ray spectra (EDS) of the Fe-28Al alloy after annealing at 1000°C for 24 h and furnace-cooling: (a) etched microsection, (b) non-etched microsection, (c) surface distribution of the elements, and (d) collation of characteristic radiation spectra for the matrix and the phase.

existence of phases with chemical composition close to that of the matrix. The obtained results (SEM) are confirmed by qualitative analysis of chemical composition, carried out by scanning transmission electron microscopy, where also the presence of iron and aluminum only was found in the identified phases. **Figure 5** presents a collation of X-ray spectra obtained by STEM for the matrix and for the investigated phase. No differences in characteristic radiation spectra for the matrix and for the phase were found, which proves comparable concentrations of elements in both studied microzones.

Then, studies using electron backscatter diffraction were carried out. The obtained pattern of Kikuchi lines of the disclosed phase is shown in **Figure 6**. An analysis of geometry of the line pattern indicated occurrence of a Fe_3Al phase in the Fe-28Al alloy. This fact was confirmed by studies of electron diffraction on a transmission electron microscope. Its results are depicted in **Figure 7**.

The results are consistent with the phase equilibrium system, because in both studied systems, the Fe_3Al phase may form during slow cooling at a temperature from approx. 500°C (for Fe-28Al) and from approx. 300°C (for Fe-38Al).

Due to the hot plastic working process planned in further steps, a structural analysis in the state after the high-temperature annealing was carried out, using rapid cooling in oil for vacancy freezing. In the case of the studied alloys, rapid cooling eliminates the formation of phase in the microstructure, exemplified in **Figure 8**. It suggests a lack of influence of the Fe_3Al phase disclosed in the heat treatment process on the planned course of the hot plastic working process in the studied alloys.

3.2. Characteristics of the selected thermal properties of alloys intended for further plastic working

Thermomechanical behavior of intermetallic alloys at a high temperature is connected with the existing state of structural ordering and with the complex defect structure, including the characteristic phenomenon of supersaturation with vacancies [1, 2]. Both the structure ordering and the presence of multiple defect types affect the properties of the studied alloys

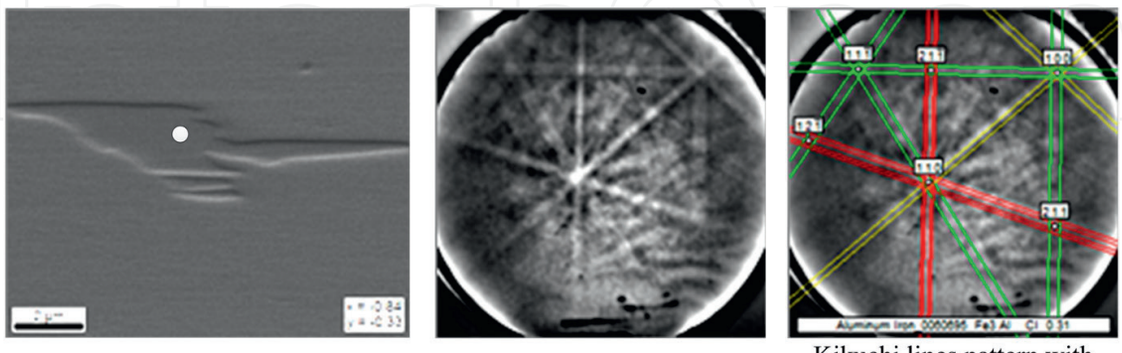

Figure 6. Results of studies of the microstructure (EBSD) of the Fe-28Al alloy after annealing at 1000°C for 24 h and furnace-cooling.

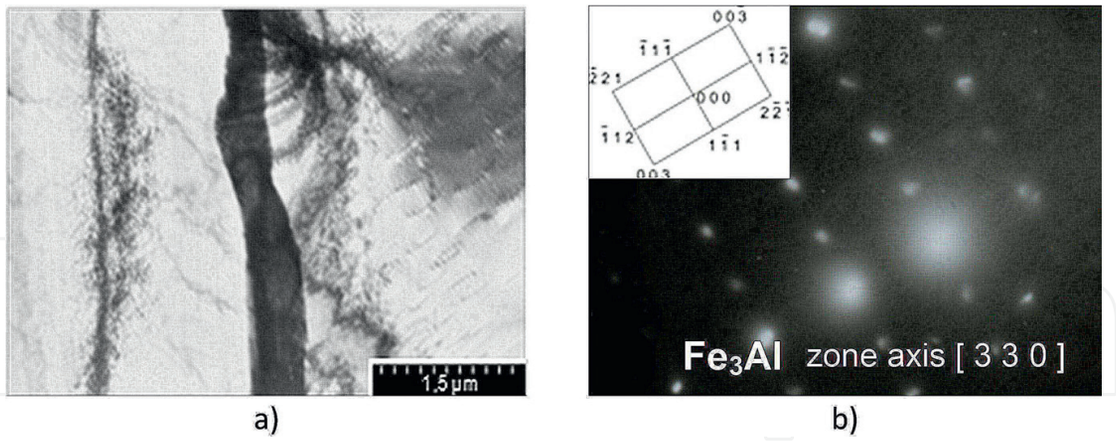

Figure 7. Microstructure of the Fe-28Al alloy after annealing at 1000°C for 24 h and furnace-cooling (TEM): (a) experimental zone (white area) and (b) diffraction pattern from the analyzed phase and diffraction solution.

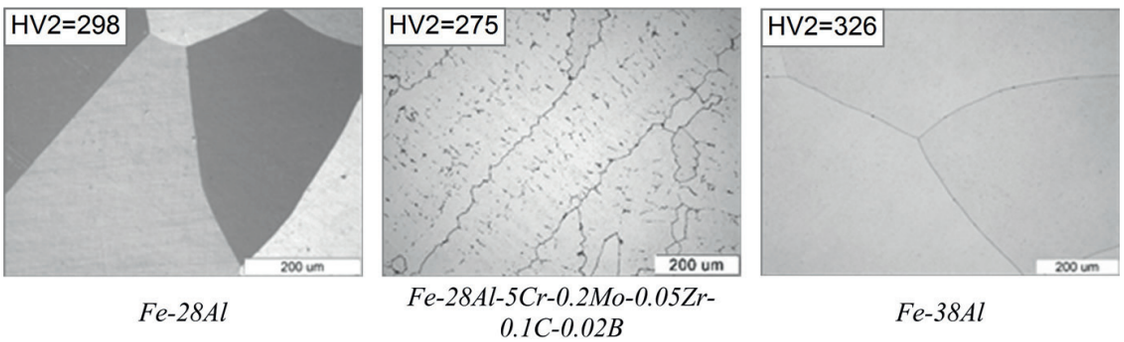

Figure 8. Microstructures of the studied alloys after the high-temperature annealing for 24 h and oil cooling.

significantly. From the point of view of the plastic working process, it is necessary to determine the characteristic temperatures in relation to changes in the ordering type and the temperature of transition into a disordered state, in which the plastic working process may be realized. Characteristic transition temperatures were determined by dilatometric method and confirmed by DTA. The results obtained for the selected alloys are gathered in **Figure 9**. Critical temperature of the change in the ordering type in the alloys with 28 at.% Al was identified, connected with the transition from the B2 ordering-type state into DO_3 at a temperature of approx. 550°C. For alloys with 38 at.% Al, a thermal effect was observed at a temperature of approx. 1260°C, which may be connected with the process of transition from a disordered (A2) into an ordered (B2) solid solution, and another one at a temperature of approx. 1060°C, which is probably a result of changes in physical properties within the phase B2 occurrence area, and precisely, with the B2(h) → B2′ transition, the changes being connected with a rebuilding of the defect structure [6].

3.3. Plastometric studies and their verification

Technological plasticity and thus the deformabilities of the studied alloys are significantly affected by the value of flow stress. In the case of the Fe-Al alloys, the more important

http://dx.doi.org/10.5772/intechopen.76701

Dilatometric analysis

	Transition temperatures				Transition temperatures	
Fe-28Al	*N [°C]*	573	1279	Fe-38Al	*N [°C]*	1310
	description	*$DO_3 \leftrightarrow B2$*	*end of the disordering process B2↔A2*		*description*	*end of the disordering process B2↔A2*
	CH [°C]	1163	522		*CH [°C]*	1286
	description	*beginning of the ordering process A2↔B2*	*$B2 \leftrightarrow DO_3$*		*description*	*beginning of the ordering process A2↔B2*

N – heating; CH – cooling

DTA analysis

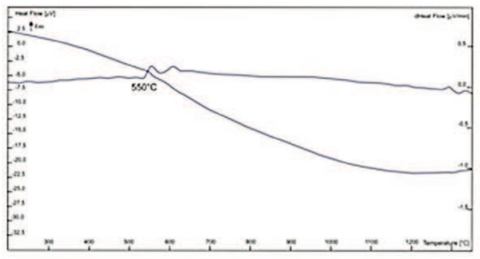

DTA curve for cooling of the Fe-28Al alloy after annealing at 1000°C/24h and furnace-cooling

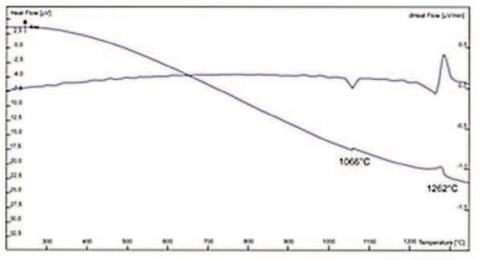

DTA curve for cooling of the Fe-38Al alloy after annealing at 1000°C/24h and furnace-cooling

Figure 9. Transition temperatures for the Fe-28Al and Fe-38Al alloys recorded by dilatometric method and differential thermal analysis method.

factors affecting their behavior during deformation at a given temperature include Al content and, consequently, the obtainable different structure types of the alloy matrix, i.e., a matrix with an ordered structure of DO_3 or B2 type. The type of the alloy matrix should be related to phase transitions, occurring with the given chemical composition, which may be used while selecting the parameters of the plastic working so as to decrease the value of flow stress at the given value of deformation. Also, the different deformation mechanism, depending on the Al content in this case, should be taken into account.

The obtained results of plastometric examinations indicate that at a temperature below 900°C, the discussed alloys undergo a strong hardening. Deformation at a higher temperature affects a decrease of the flow stress value (**Figure 10**). A tendency to increase the hardening with the increasing Al content was found in the plastometric tests. The highest σ_p values among the studied alloys are exhibited by the Fe-38Al alloy.

Analysis of the shape of the flow curves and evaluation of the structure of the studied alloys indicated that the prevailing rebuilding mechanism of the defected structure changes depends on the Al content. In alloys containing 28 at.% Al, a phenomenon of grain defragmentation is

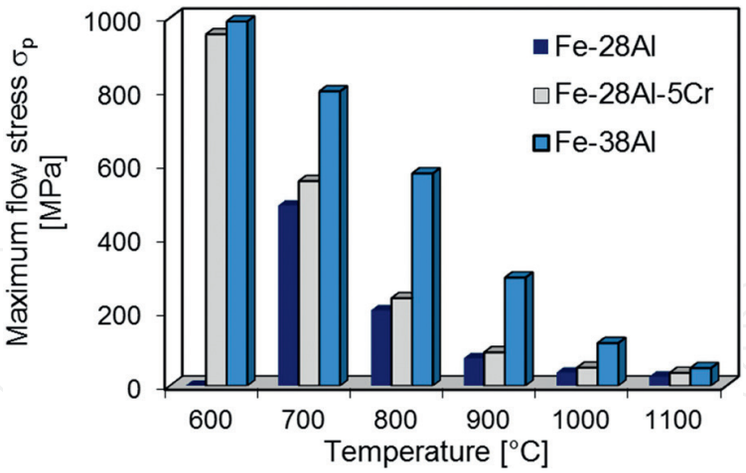

Figure 10. Influence of the deformation temperature on maximum flow stress of the studied alloys (deformation rate 1 s^{-1}).

observed in the microstructure (**Figure 11**). Inside the primary grains, new grains nucleate. In the substructure, climb of dislocation, polygonization, and subgrain coalescence prevail phenomena characteristics for dynamic recovery process (**Figure 12**). In alloy with a higher Al content, prevalence of the wide-angle migration process of the grain boundaries and formation of new grains and phenomena accompanying the process of stricture rebuilding in the result of dynamic recrystallization were observed (**Figures 11** and **13**).

After plastometric studies, rolling tests under laboratory conditions were carried out. Ingots of Fe-28Al, Fe-28Al-5Cr, and Fe-38Al alloys having dimensions of approx. 160 × 30 × 20 mm (**Figure 2**) after homogenizing annealing constituted charge materials. Hot rolling was carried out on a two-high reversed rolling mill with roller diameter of 65 mm at VSB-TU Ostrava. The samples were heated to a temperature of 1150°C and then rolled in three roll passes. The following percentage reductions were applied: 15, 15, and 15%. Rotational speed of the rollers was 80 rpm. After rolling, the samples were cooled in air. The process was carried out for ingots without covers and using covers made of ferritic steel (AISI 430) in order to protect the alloy surface from oxidation and cracking in the result of contact with cold rollers. In **Figure 13**, views of obtained profiles are collated. It was observed that in the case of binary alloys, it was necessary to use covers during hot rolling. A particularly evident net of deep cracks was observed after

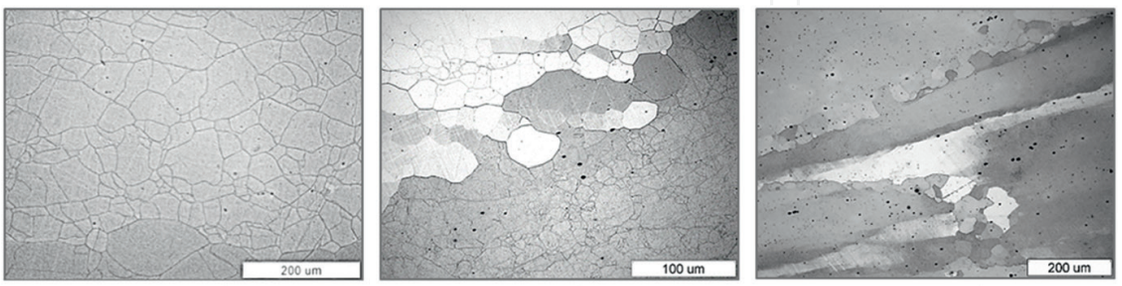

Figure 11. Microstructures of the alloys after deformation with a rate of 0.1 s^{-1} at T = 1000°C.

http://dx.doi.org/10.5772/intechopen.76701

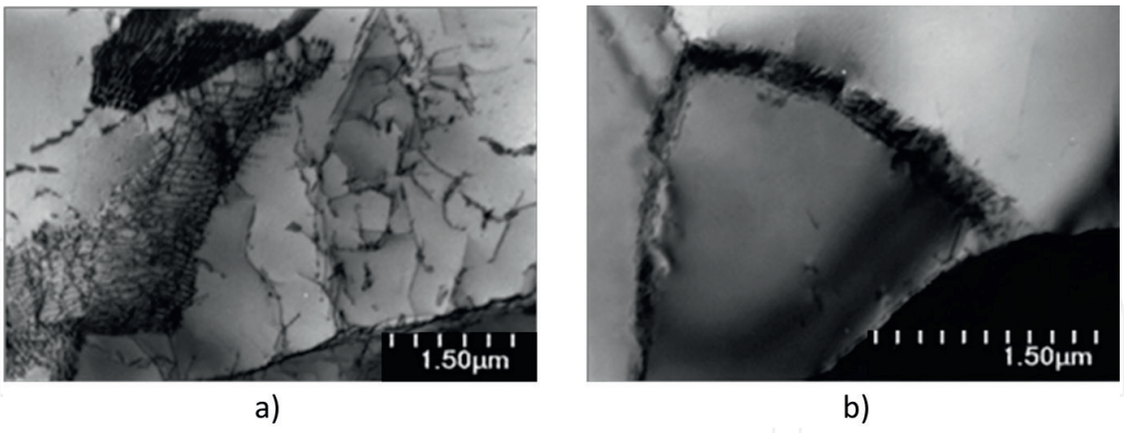

Figure 12. Substructure of the Fe-28Al alloy after deformation with a rate of 0.1 s^{-1} at T = 1000°C: (a) subgrain structure and (b) dislocation rearrangement-polygonization effect.

rolling without covers in the Fe-38Al alloy. In the case of the Fe-28Al-5Cr alloy, a qualitatively good surface was obtained even after rolling without covers (**Figure 14**).

For selected flats, a further rolling process was carried out using percentage reductions 15, 15, and 15% to a thickness of 6 mm, obtaining semifinished products (**Figure 15**) of satisfactory quality.

Then, tests of corrosion resistance in the "acid rain" environment – pH = 3.5 and 3% NaCl aqueous solution, for samples after homogenizing annealing and rolling was carried out. The scope of the tests included potentiostatic, galvanostatic, and potentiodynamic examinations as well as investigation of the condition of the sample surface after corrosion. It was proven that, in most cases, the tested alloys are characterized by a tendency for activation (depassivation) of the surface under the aforementioned conditions. The best corrosion resistance was exhibited by samples of the Fe-38Al alloy. For the samples of this alloy, the lowest values of current density for a potential both of $E = E_{kor} + 300$ mV and $E = E_{kor} + 500$ mV were recorded. A significant increase in the current density from the value of the corrosion current density to the value of the current density for the potential of $E = E_{kor} + 300$ mV was characterized here. Comparing the tests results for the samples

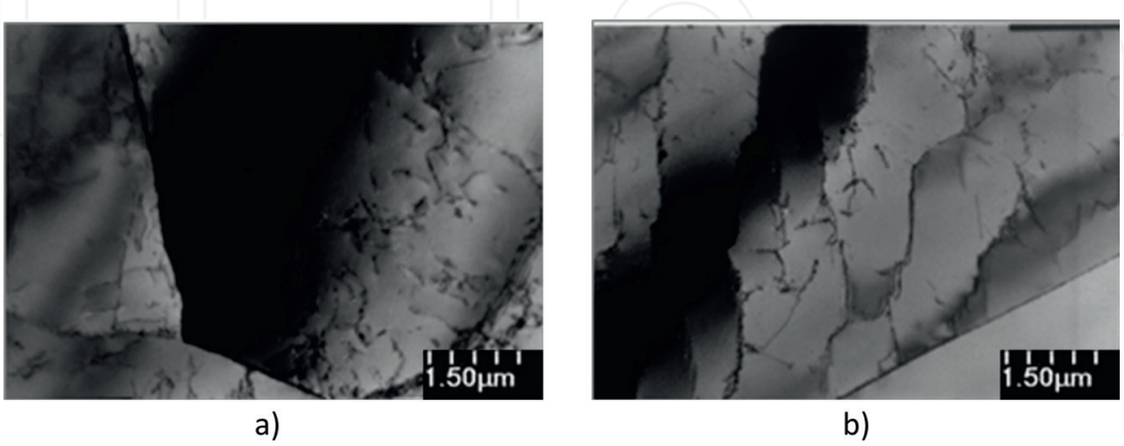

Figure 13. Substructure of the Fe-38Al alloy after deformation with a rate of 1 s^{-1} at T = 1000°C: (a) wide-angle boundaries migration and (b) subgrain structure with a diversified dislocation density.

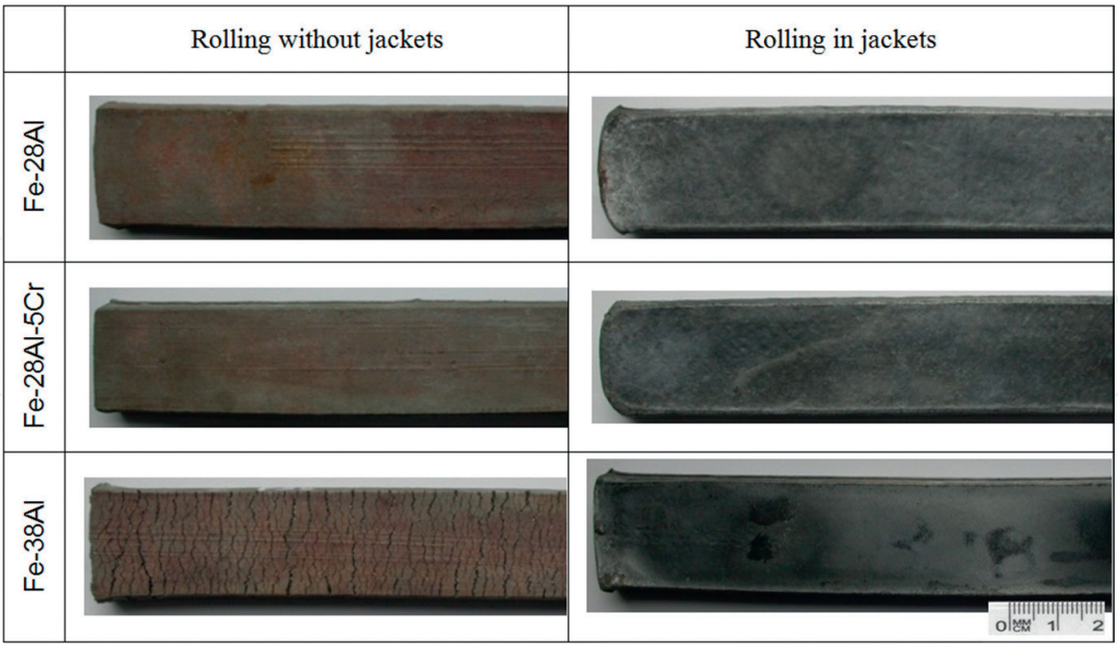

Figure 14. Photographs of surfaces of the flats obtained after hot rolling.

Figure 15. Views of the profiles after rolling with total reduction of ~70% to a thickness of 6 mm.

with various degrees of deformation, one may see that a higher deformation degree under nonstationary conditions, or those closer to the actual corrosion conditions, does not cause an acceleration of the corrosion but, unlike under stationary conditions, a slowdown. For all studied alloys, the corrosion has a local character and leads to the formation of small point pits (**Figure 16**).

The studies carried out hitherto allowed for ascertaining that further technological tests should be carried out for the alloy with 38 at.% Al content. However, realization of tests for the alloy with such aluminum content with microadditions was planned at this stage. It was imposed, most of all, by the role of microadditions in the hardening process of grain boundaries.

Realizing the planned research program intended for obtaining semifinished products in the form of thin sheets, a sheet production process from the Fe-38Al-0.2Mo-0.05Zr-0.1C-0.02B alloy was applied, consisting of heat treatment and plastic working. A semifinished product with a thickness of ~2 mm (**Figure 17**) was obtained.

http://dx.doi.org/10.5772/intechopen.76701

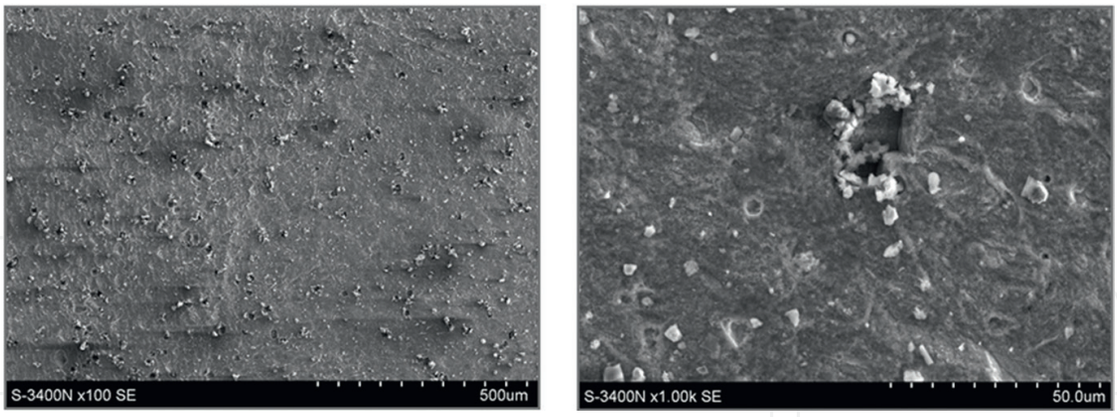

Figure 16. Surface of the Fe-38Al alloy (condition after rolling with a total reduction of ~70% to a thickness of 6 mm) after corrosion tests.

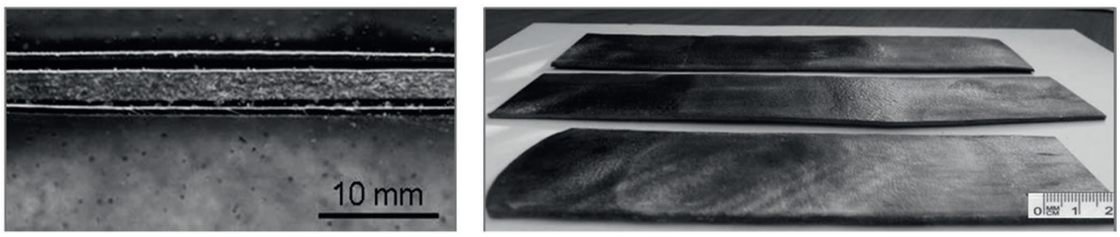

Figure 17. Flats made of the Fe-38Al-0.2Mo-0.05Zr-0.1C-0.02B alloy.

Successful results of the realized rolling tests induced realization of further planned goals, i.e., preparation of bars from the tested alloy by two techniques: rolling and hydrostatic extrusion. Execution of these tests was planned using metal covers.

Rolling of ingots from the Fe-38Al-0.2Mo-0.05Zr-0.1C-0.02B alloy with initial diameters of Ø30 mm and Ø22 mm (**Figure 2**) was carried out on a three-high mill. Before the rolling, the ingots were heated for approx. 45 min; the heating temperature was higher by 30°C than the planned initial rolling temperature, i.e., 1250°C. The rolling was carried out without reheating. In the first step, rolling of the ingots to a diameter of Ø12 mm was planned. **Figure 18**

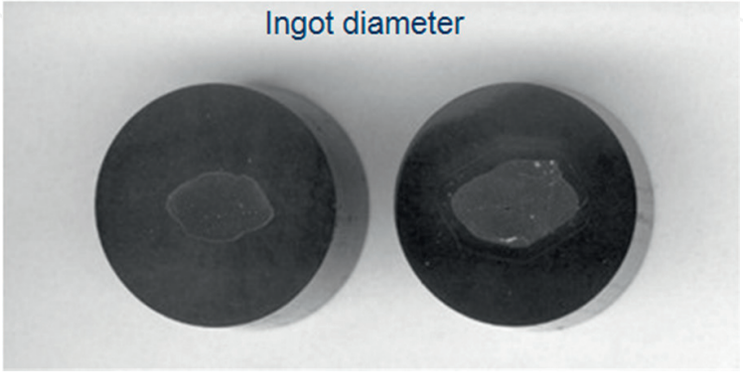

Figure 18. Cross sections of the bars formed in the hot rolling process (uncontrolled material flow).

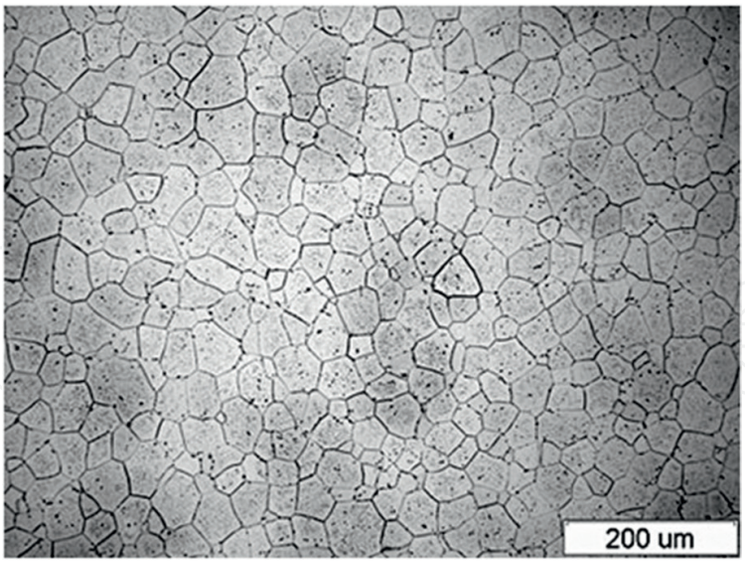

Figure 19. Microstructure of the Fe-38Al-0.2Mo-0.05Zr-0.1C-0.02B alloy after the hot rolling process.

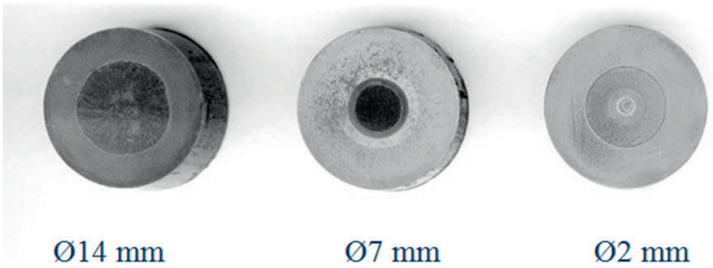

Figure 20. Cross sections of the bars formed in the hot hydrostatic extrusion process.

shows cross sections of the produced bars. Considering the occurrence of an uncontrolled material flow, further reduction of the cross section was canceled. However, it should be emphasized that in spite of the technological difficulties, a homogeneous and fine-grained structure was obtained (**Figure 19**).

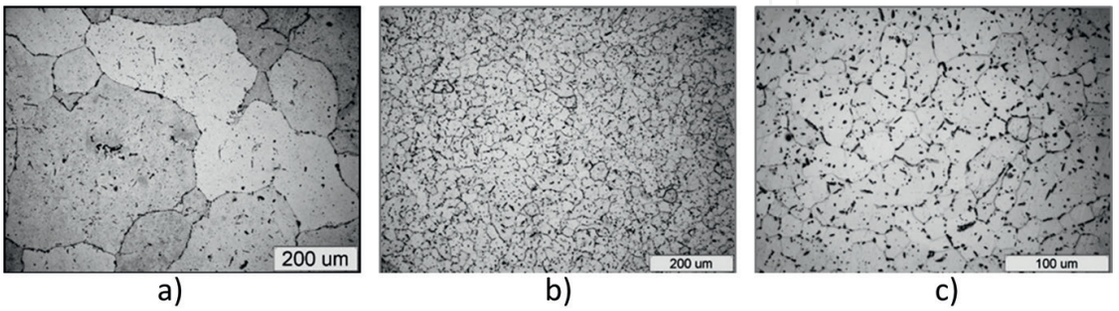

Figure 21. Microstructure of the Fe-38Al-0.2Mo-0.05Zr-0.1C-0.02B alloy: (a) after casting and heat treatment and (b–c) after the hot hydrostatic extrusion process (diameter 2 mm).

http://dx.doi.org/10.5772/intechopen.76701

The hot hydrostatic extrusion process was carried out for an ingot of the Fe-38Al-0.2Mo-0.05Zr-0.1C-0.02B alloy, having a diameter of 30 mm after homogenization at a temperature of 1000°C. Cross sections of the prepared bars are shown in **Figure 20**.

An effective structure refinement was obtained after the hydrostatic extrusion process. **Figure 21** presents the alloy microstructure after the homogenization process and after the extrusion process.

4. Summary and conclusions

The tests carried out proved that melting of the studied alloys in induction vacuum furnaces is technically possible while maintaining the given process parameters. In the results of the application of the charge in the form of very pure components, melting and single refinement remelting, alloys with an assumed chemical composition, and a very low total content of gaseous impurities of the order of several ppm are obtained. It was found that the produced alloys are characterized by a very low castability and a high casting shrinkage (from 3.30 to 3.40%), leading to a coarse-grained primary structure and occurrence of shrink-type defects being deposited in the ingots.

In the process of heat treatment, during cooling, Fe_3Al phase forms in the studied alloys. According to the phase equilibrium system, the Fe_3Al phase may form during slow cooling at a temperature from approx. 500°C (for Fe-28Al) and from approx. 300°C (for Fe-38Al). In order to eliminate the influence of the Fe_3Al phase disclosed in the heat treatment process on the planned hot plastic working process, a heat treatment operation with oil cooling was used for the studied alloys to freeze the structure. Therefore, lack of influence of the aforementioned phase on the deformation process was confirmed.

From the point of view of the plastic working process, it was necessary to determine the characteristic temperatures in the studied alloys, particularly in relation to the changes in the ordering type and the temperature of transition into a disordered state, in which the plastic working process could be realized. Critical temperature of the change in the ordering type in the alloys with 28 at.% Al was identified, connected with a transition from the ordered state of B2 type into DO_3 type at a temperature of approx. 550°C. For alloys containing 38 at.% Al, a temperature of transition from a disordered (A2) into an ordered (B2) solid solution was identified, and temperatures of transitions are connected with a rebuilding of the defect structure within the B2 phase.

The obtained results of the plastometric studies indicated possibilities of technological forming of the studied alloys in the temperature range from 900 to 1200°C. At a lower temperature, strong hardening renders the deformation process more difficult. The technological hot plastic forming tests proved a possibility to obtain flat hot-rolled products consistent with the assumptions while maintaining the final rolling temperature not lower than 950°C, using metal covers. A proper method for production of bars consistent with the assumptions is the high-temperature hydrostatic extrusion process. A product obtained by this method warrants meeting the dimensional requirements, which has not been obtainable by rolling. In the case of both technologies applied, manufacturing of products in the form of bars requires an additional operation for jacket removal.

5. Possible applications

Potentially, the use of the developed flat products in heating systems of heat exchangers as substitutes for stainless steels used hitherto may be planned. Moreover, application of the developed products in the form of bars as elements of operational systems of motor vehicles may be envisaged, including particularly the use for roller axles of the supercharging pressure system of turbo.

Author details

Magdalena Jabłońska*, Iwona Bednarczyk, Anna Śmiglewicz and Tomasz Mikuszewski

*Address all correspondence to: magdalena.jablonska@polsl.pl

Silesian University of Technology, Faculty Materials Engineering, Institute of Materials Engineering, Katowice, Poland

References

[1] Wolff J, Franz M, Broska A, Kerl R, Weinhagen M, Köhler B, Brauer M, Faupel F, Hehenkamp T. Intermetallics. 1999;**7**:289-300. DOI: 10.1016/S0966-9795(98)00105-8

[2] De Diego N, Plazaola F, Jiménez JA, Serna J, del Río J. Acta Materialia. 2005;**53**:163-172. DOI: 10.1016/j.actamat.2004.09.013

[3] Stoloff NS. Materials Science and Engineering. 1998;**A258**:1-14. DOI: 10.1016/S0921-5093(98)00909-5

[4] Kratochvil P, Schindler I. Intermetalics. 2007;**15**:436-438. DOI: 10.1016/j.intermet.2006.06.005

[5] Schindler I, Kratochvil P, Prokopcakova P, Kozelsky P. Intermetallics. 2010;**18**:745-747. DOI: 10.1016/j.intermet.2009.11.005

[6] Kerl R, Wolff J, Th H. Intermetallics. 1999;**7**:301-308. DOI: 10.1016/S0966-9795(98)00118-6

[7] Pike LM, Liu CT. Intermetallics. 2000;**8**:1413-1416. DOI: 10.1016/S0966-9795(00)00095-9

[8] Baligidad RG, Radhakrishna A. Materials Science and Engineering. 2001;**A308**:136-142. DOI: 10.1016/S0921-5093(00)02026-8

[9] Cizek J, Lukac F, Melikhova O, Prochazka I, Kuzel R. Acta Materialia. 2011;**59**:4068-4078. DOI: 10.1016/j.actamat.2011.03.031

[10] Salazar M, Albiter A, Rosas G, Pérez R. Materials Science and Engineering. 2003;**A351**:154-159. DOI: 10.1016/S0921-5093(02)00825-0

[11] Jabłońska MB, Mikuśkiewicz M, Śmiglewicz A, Bernstock-Kopaczyńska E. Defect and Diffusion Forum. 2012;**326-328**:573-577. DOI: 10.4028/www.scientific.net/DDF.326-328.573

[12] Jabłońska M, Hanc A, Szostak A. Solid State Phenomena. 2010;**163**:299-302. DOI: 10.4028/www.scientific.net/SSP.163.299

[13] Jabłońska M, Jasik A, Hanc A. Archives of Metallurgy and Materials. 2009;**54**:731-739

[14] Massalski TB editor. ASMM, Metals Park, O. 1986. p. 234

[15] Anton DL, Shah DM. High temperature ordered intermetallic alloys IV. In: Johnson LA, Pope DP, Stiegler JO, editors. Mater. Res. Soc. Proc. 213. Pittsburgh, PA; 1991. p. 733

[16] Fraczkiewicz A, Gay AS, Biscondi M. Materials Science and Engineering. 1998;**A258**:108. DOI: 10.1016/S0921-5093(98)00923

[17] Morris MA, Morris DG. Scripta Materialia. 1998;**38**:509. DOI: 10.1016/S1359-6462(97)00468-5

[18] Konrad J, Zaefferer S, Schneider A, Raabe G, Frommeyer G. Intermetallics. 2005;**13**: 1304-1312. DOI: 10.1016/j.intermet.2004.10.01

[19] Kobayashia S, Zambaldib C, Raabe D. Acta Materialia. 2010;6672-6684. DOI: 10.1016/j.intermet.2004.10.017

[20] Schindler I, Kopeček J, Kawulok P, Jabłońska M, Hadasik E, Jóźwik P, Opěla P, Hanus P, Polkowski W, Bojar Z. Archives of Civil and Mechanical Engineering. 2017;**17**(4): 816-826. DOI: 10.1016/j.acme.2017.03.004

[21] Li D, Lin D, Liu Y. Materials Science and Engineering. 1998;**A249**:206-216. DOI: 10.1016/S0921-5093(98)00507-3

[22] Łyszkowski R, Bystrzycki J. Intermetallics. 2006;**14**:1231-1236. DOI: 10.1016/j.intermet.2005.12.014

[23] Reimann U, Sauthoff G. Intermetallics. 1999;**7**:437-441. DOI: 10.1016/S0966-9795(98)00104-6

[24] Łyszkowski R, Bystrzycki J, Płociński T. Intermetallics. 2010;**18**:1344-1349. DOI: 10.1016/j.intermet.2009.12.026

[25] Dolata A, Śleziona J, Formanek B. Journal of Materials Processing Technology. 2006;**175** (1-3):192-197. DOI: 10.1016/j.jmatprotec.2005.04.015

[26] Karczewski K, Jóźwiak S, Bojar Z. Archives of Metallurgy and Materials. 2007;**52**:361-365

[27] Cebulski J, Basa J, Pasek D. Solid State Phenomena. 2014;**212**:49-52. DOI: 10.4028/www.scientific.net/SSP.212.49

[28] Łyszkowski R, Bystrzycki J. Materials Characterization. 2014;**96**:196-205. DOI: 10.1016/j.matchar.2014.07.004

IntechOpen